Neurobehavioural signatures of learning that emerge in a real-world motor skill task

Shlomi Haar[1,2], Camille M. van Assel[1] & A. Aldo Faisal[1,2,3,4]

1. Brain & Behaviour Lab, Dept. of Bioengineering, Imperial College London, London, UK.
2. Behaviour Analytics Lab, Data Science Institute, London, UK.
3. Dept. of Computing, Imperial College London, London, UK.
4. Medical Research Council London Institute of Medical Sciences, London, UK.

Corresponding authors: Shlomi Haar (s.haar@imperial.ac.uk) and Aldo Faisal (aldo.faisal@imperial.ac.uk) Imperial College London, London, SW7 2AZ, UK

Keywords: motor learning, motor skill, real-world, full-body movement, EEG, Post-movement beta, movement variability, motor neuroscience

Conflict of Interest: The authors declare no competing financial interests.

Contributions: SH and AAF conceived and designed the study; SH and CVA acquired and analyzed the data; SH and AAF interpreted the data; SH drafted the paper; SH and AAF revised the paper

Acknowledgements: We thank our participants for taking part in the study. We acknowledge the technical support by Alex Harston and Chaiyawan Auepanwiriyakul. We also thank Alex Harston for helpful comments on the manuscript. The study was enabled by financial support to a Royal Society-Kohn International Fellowship (NF170650) and by eNHANCE (http://www.enhance-motion.eu) under the European Union's Horizon 2020 research and innovation programme grant agreement No. 644000 (SH, AAF).

Abstract

The behavioral and neural processes of real-world motor learning remain largely unknown. We demonstrate the feasibility of human neuroscience in-the-wild using wearables for naturalistic full-body motion tracking and mobile brain imaging to study motor learning in billiards. Motor learning in-the-wild displays well-known features of reductionistic toy-tasks, such as multiple learning rates, generalization, and the relationship between motor variability and motor learning. However, we find that real-world motor learning affects the whole body, changing motor control from head to toe. Moreover, we discovered two groups of learners, not resolved before in toy-tasks. EEG dynamics of post-movement Beta rebound (PMBR) increase in the first but decrease in the second. Behaviorally, only the second group controls task-relevant variability dynamically and learns faster. We speculate that these groups emerge because subjects must combine multi-modal mechanisms of de-novo motor controller learning and motor adaptation in new ways when faced with the complexity of the real-world.

Introduction

Motor learning is a key feature of our development and daily lives, from a baby learning to roll, to an adult learning a new sport, or a patient undergoing rehabilitation after a stroke. The process of learning a real-world motor skill is usually long and complex, and difficult to quantify. As a result, real-world motor learning is rarely studied, and most of the motor learning literature focuses on relatively simple tasks, performed in a lab setup or an MRI scanner, such as force-field adaptations (e.g. Diedrichsen et al., 2005; Howard et al., 2015; Shadmehr and Mussa-Ivaldi, 1994; Smith et al., 2006), visuomotor perturbations (e.g. Haar et al., 2015; Krakauer et al., 2000; Mazzoni and Krakauer, 2006; Taylor et al., 2014), and sequence-learning of finger tapping or pinching tasks (Clerget et al., 2012; Ma et al., 2011; Reis et al., 2009; Yokoi et al., 2018).

These reductionistic toy-tasks enable us to isolate specific features of the motor learning and tackle them individually. While this plays an important role in our understanding of sensorimotor control and learning, it address a very restricted range of behaviors that do not capture the full complexity of real-world motor control and may overlook fundamental principles of motor control and learning in real-life (Ingram and Wolpert, 2011; Wolpert et al., 2011). To tackle this, we applied naturalistic approaches and developed a Bioinformatics of Behavior database (Faisal et al., 2010) of real-world motor learning behavior. Unlike the few previous studies that used real-world tasks (such as juggling), which focused on anatomical and functional MRI changes due to learning and did not record behavior or neural activity during the learning process (e.g. Hecht et al., 2014; Ono et al., 2015; Sampaio-Baptista et al., 2014, 2015; Scholz et al., 2009), our Bioinformatics of Behavior database includes the full body movement and EEG brain activity during the entire learning period, as well as the measurements of task performance. This enables us to quantify the trends of changes in each of them separately, during the entire learning process, and to look for correlations between the physiological measures and reveal neurodynamical processes behind motor learning.

Here we are taking novel data-driven approaches to study behavior where it matters most – in natural, real life settings (Ingram and Wolpert, 2011). It is only in natural behavioral settings that neuroscientific mechanisms are subject to evolutionary selection pressures and it is the operation in these contexts for which the nervous system has been designed (Hecht et al., 2014). The paradigm in which we study real-world motor learning is the game of pool table billiards. Billiards is a real-world task ideally suited to neurobehavioral study as motion tracking in terms of movement in space, the natural constraints of game play, and divisibility into trials captures the style of reductionistic lab-based motor learning tasks. Billiards is also a natural task which is complex and involves many different sub-tasks (precision, alignment, ballistic movements, high-level sequential planning) which requires complex skills. To the best of our knowledge, this is the

first study to record both the behavior and the neural responses throughout the entire process of real-world motor learning.

We structure the results as follows: We ground our results in previous work on reductionistic lab tasks, to show that our unconstrained task and its task goal (directional error of the target ball relative to the pocket it is meant to go in) displays the well-known features of human motor learning. We then characterize full-body movement structure during the task, and how learning changes over trials the kinematics of all joints. Next, we compare across subjects to map their performance, learning rates, and motor variability, and how initial variability and learning rates are linked. We then relate the EEG activity during the trials which reveals two groups of learners with different PMBR dynamics and learning characteristics. We address the neural and behavioral differences between the two groups which are suggestive of differences in the learning mechanisms employed by the subjects.

Results

20 right-handed volunteers, with little to no previous experience playing billiards, performed 300 repeated trials (6 sets of 50 trials each with short breaks in-between) where the cue ball and target ball were placed in the same locations, and subjects were asked to shoot the target ball towards the far-left corner pocket, followed by additional 100 trials (2 sets of 50 trials each) where the balls were placed in their same respective locations, and the subjects were asked to shoot instead towards the far-right corner pocket (Figure 1A). During the entire learning process, we recorded the subjects' full body movements with a 'suit' of inertial measurement units (IMUs; Figure 1B), and their brain activity with wireless EEG (Figure 1C).

Movement and Learning in a real-world pool task

The balls on the pool table were tracked with a high-speed camera to assess the outcome of each trial (Figure 1D). The ball tracking data shows a double exponential learning curve for the decay in the directional error of the target ball (relative to the direction from its origin to the center of the target pocket) over trials (Figure 1E). The direction of the initial trials error was consistent across subject as they tended to hit the center of the target ball and shot it forward towards the center of the table. On the trial to the second target (trials 300-400) subjects showed the same trend of shooting initially towards the center of the table and therefore the directional error relative to the pocket is negative. For measuring suc

cess rates and intertrial variability we divided the trials into blocks of 25 trials each (each experimental set of 50 trials was divided to two blocks to increase the resolution). Since learning occurs within block (especially during the first block) and the variability might be driven by the learning gradient, we corrected for it by calculating intertrial variability over the residuals from a

regression line fitted to the ball direction in each block. The learning curve over blocks (Figure 1F) emphasize the reduction in the inter-subject variability during learning (decreasing error bars) and the increase in the average absolute error back to its initial values on the first block to the second target. The success rate over blocks (percentage of successful trials in each block; Figure 1G) shows similar learning to the directional error.

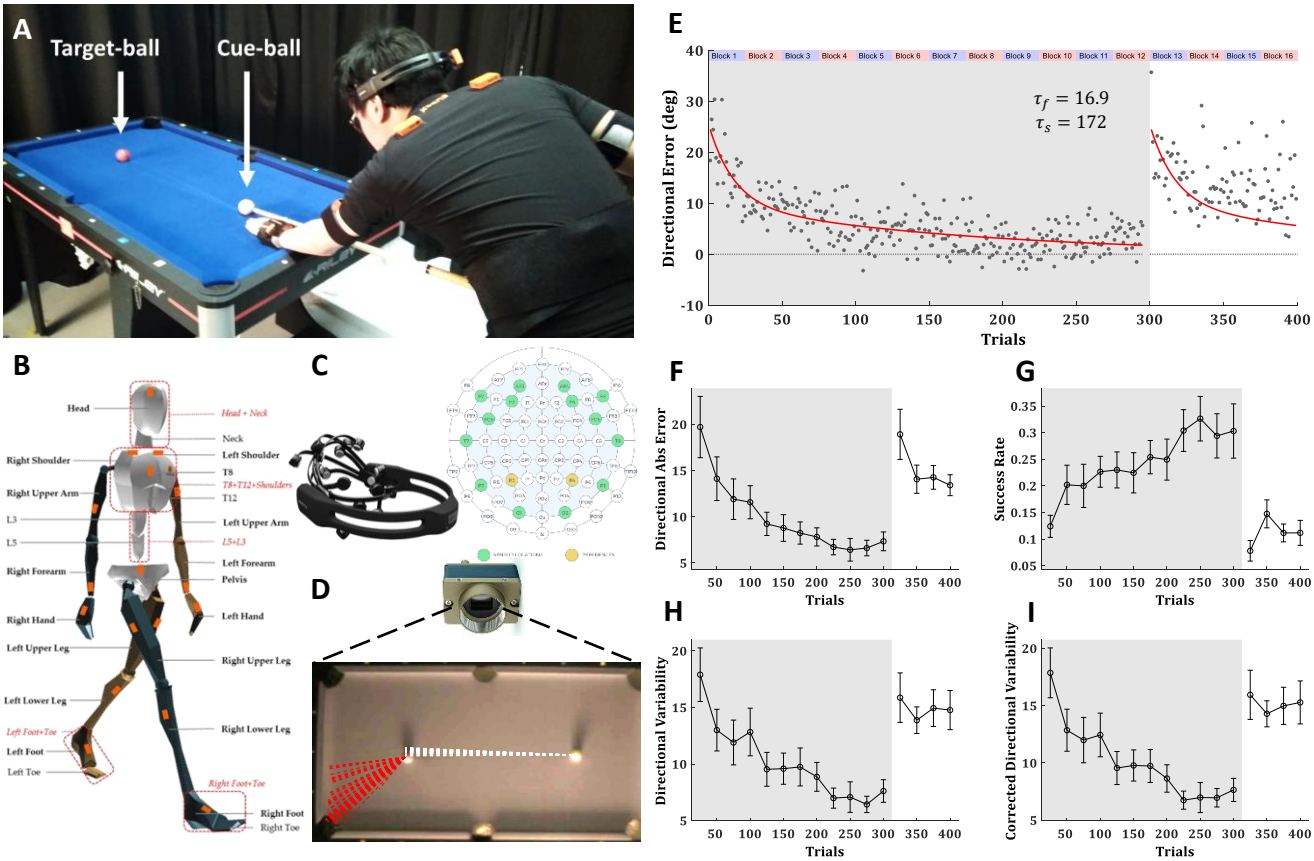

Figure 1. *Experimental setup and paradigm and Task learning*. (**A**) 20 right-handed healthy subjects played pool table billiards. They performed 300 repeated trials towards the far-left corner followed by an additional 100 trials towards the far-right corner. (**B**) Full body movement was recorded with a 'suit' of 17 wireless IMUs (Xsens MVN Awinda). (**C**) Brain activity was recorded with a 14 channels wireless EEG system (eMotiv EPOC+). (**D**) The balls were tracked with a high-speed camera. Dashed lines show the trajectories of the cue (white) and target (red) balls over 50 trials of an example subject. (**E**) The trial-by-trial directional error of the target-ball (relative to the direction from its origin to the centre of the target pocket) for the first (grey background) and the second (white background) target, averaged across all subjects, with a double-exponential fit (red curve). The trials to the second target are presented with the curve of the fit to the first target. (**F**) The mean absolute directional error of the target-ball (**G**) The success rate, (**H**) directional variability, and (**I**) directional variability corrected for learning (see text). (**F-H**) presented over blocks of 25 trials for the first (grey background) and the second (white background) target, averaged across all subjects, error bars represent SEM.

The learning is also evident in the intertrial variability in the shooting direction (Figure 1H) which decays over learning and jumps back up after changing targets. Corrected intertrial variability (Figure 1I) was calculated over the residuals from a regression line fitted to the ball direction in each block, to correct for the learning that is happening within the block, and showed the same pattern. All these graphs suggest that subjects reached their peak performance on the fifth experimental set (blocks 9-10, trials 200-250) and are doing the same or even slightly worse on the last experimental set to the first target (blocks 11-12, trials 250-300). Thus, we refer to the last two experimental sets to the first target (blocks 9-12, trials 201-300) as the 'learning plateau'.

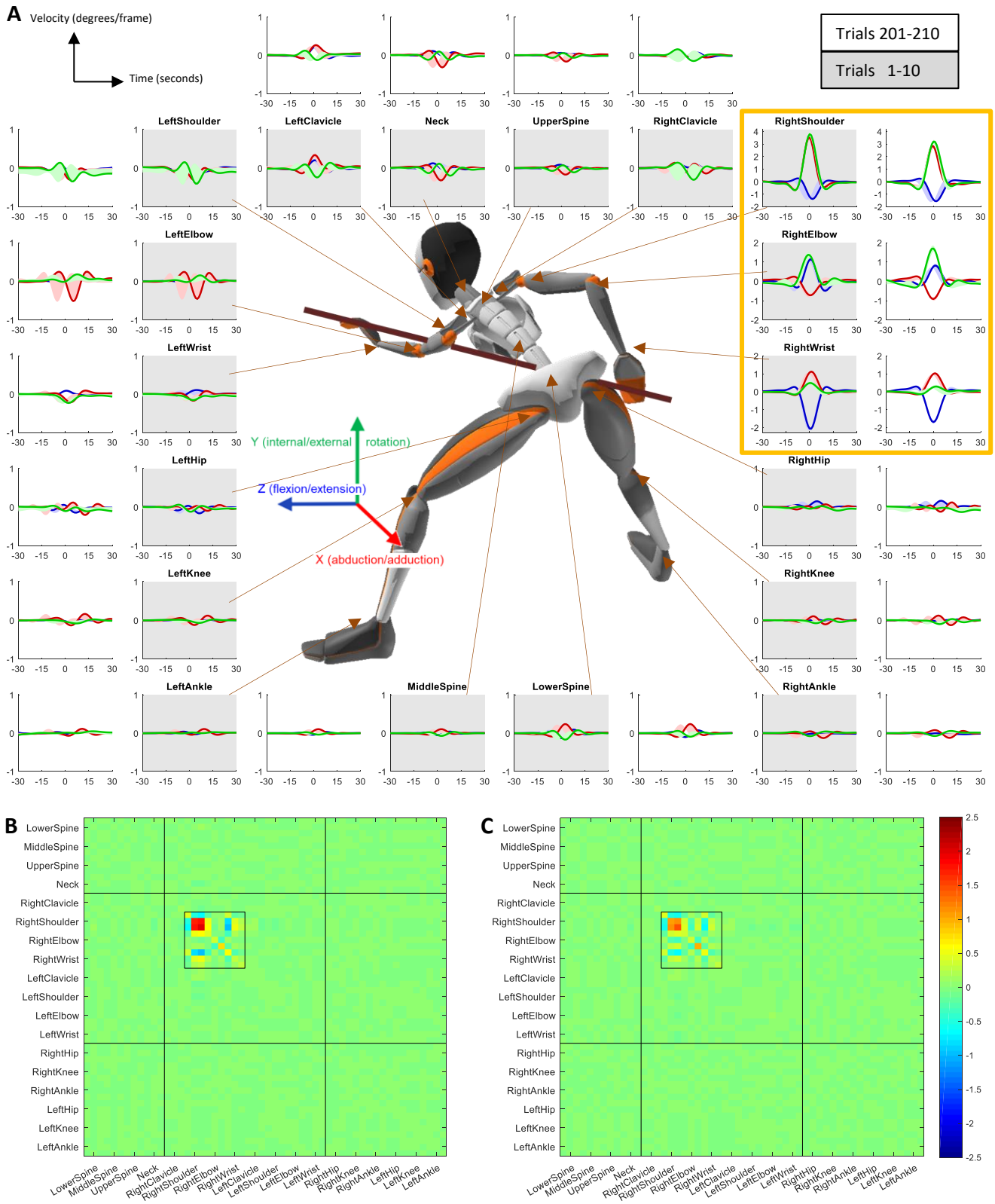

Figure 2. *Velocity profiles and covariance*. (**A**) Velocity profiles in 3 degrees of freedom for each joint (blue: flexion/extension, red: abduction/adduction; green: internal/external rotation) averaged across subjects and trials over the initial trials (1-10) in the inner circle (grey background) and after learning plateau (201-210) in the outer circle (white background). The joints of the right arm, which do most of movement in the task, are highlighted in orange box. (**B,C**) The variance covariance matrix of the velocity profiles of all joints averaged across subjects and trials (**B**) over the initial trials (1-10) and (**C**) after learning plateau (201-210).

The full body movements were analyzed over the velocity profiles of all joints, and not the joint angles profiles, as those are less sensitive to potential drifts in the IMUs and have proven to

be more robust and reproducible across subjects in natural behavior (Thomik, 2016). In the current data we can also see this robustness across trials (Figure 2A; see Fig 2A Supplement for joint angles profiles).

The covariance of the velocity profiles, averaged across the initial ten trials of all subjects, shows that most of the variance in the movement is in the right arm, and specifically in the right shoulder (Figure 2B). This is a signature for the naivety of the subjects, as pool billiards guide books emphasize that the shooting movement should be from the elbow down while the shoulder should be kept still. The covariance of the velocity profiles over ten trials after learning plateau (trials 201-210) shows similar structure and an overall decrease relative to the initial trials (Figure 2C). Velocity profiles of all joints (and especially for the joints of the right arm that carry most of the movement variance) have not changed much following learning, except from the flexion/extension of the right elbow that showed a significant decrease in velocity from the initial trials to the trials after learning plateau (Figure 2A).

The generalized variance (GV; defined as the determinant of the covariance matrix (Wilks, 1932)) over the velocity profiles of all joints increases fast over the first ~30 trials and later decreases slowly (Figure 3A), suggesting active control of the exploration-exploitation trade-off. The covariance over the initial trials, the trials over the peak GV, and trials after learning plateau (Figure 3B), shows that the changes in the GV were driven by an increase in the variance of all DoFs of the right shoulder, and a decrease in the covariance between the abduction/adduction and the internal/external rotation of the right shoulder to the flexion/extension of the right shoulder and wrist. The internal/external rotation of the right elbow shows a continuous increase in its variance, which does not follow the trend of the GV. Principal component analysis (PCA) across joints for the velocity profiles per trial for each subject, shows a slow but consistent rise in the number of PCs that explain more than 1% of the variance in the joint velocity profiles (Figure 3C). On the trials to the second target, the curve is steeper, suggesting generalization. The manipulative complexity (Belić and Faisal, 2015) shows the exact same trend (Figure 3D), which suggests that over trials subjects use more degrees of freedom in their movement.

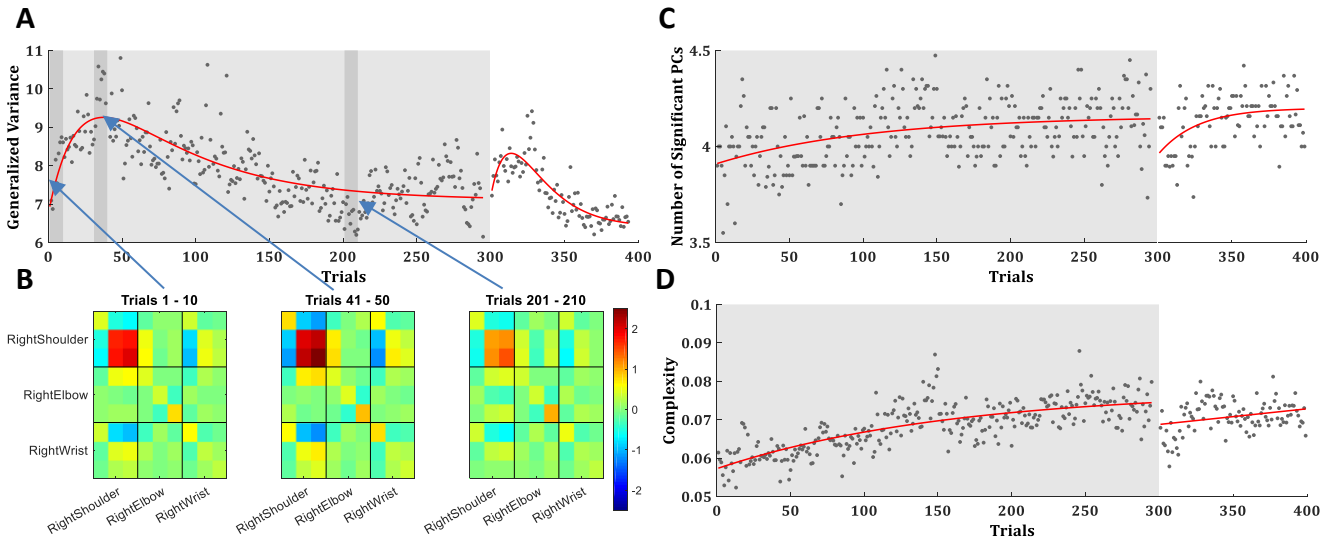

Figure 3. *Variance and Complexity*. (**A**) The trial-by-trial generalized variance (GV), with a double-exponential fit (red curve). (**B**) The variance covariance matrix of the right arm joints velocity profiles averaged across subjects and trials over the initial trials (1-10), the peak GV trials (41-50) and after learning plateau (201-210). The color bar is the same as in Figure 2. (**C**) The number of principal components (PCs) that explain more than 1% of the variance in the velocity profiles of all joints in a single trial, with an exponential fit (red curve). (**D**) The manipulative complexity (Belić and Faisal, 2015), with an exponential fit (red curve). (**A,C,D**) Averaged across all subjects, over all trials for the first (grey background) and the second (white background) target.

As a measure of task performance in body space, correlation distance was calculated between the velocity profile of each joint in each trial to the velocity profile of that joint in all successful trials to the same target. The mean over these correlation distances produces a single measure of Velocity Profile Error (VPE) for each joint in each trial.

$$VPE_i = \frac{\sum_s^{N_{scs}} corrDist(velProf_i, velProf_s)}{N_{scs}}$$

Thus, VPE in trial i is the sum of the correlation distance between the velocity profile in trial i and the velocity profile in successful trial s, divided by the number of successful trials (N_{scs}). For all joints, VPE shows a clear pattern of decay over trials in an exponential learning curve (Figure 4A). A proximal-to-distal gradient in the time constant of these learning curves is observed across the right arm, from the shoulder through the elbow to the wrist rotation which shows very slow learning (the other wrist angles had very low VPE from the start, thus do not learn much). Intertrial variability in joint movement was measured over the VPEs in each block. Learning was also evident in the VPE intertrial variability of most joints across the body (Figure 4B) that decayed over learning and jumped back after changing targets.

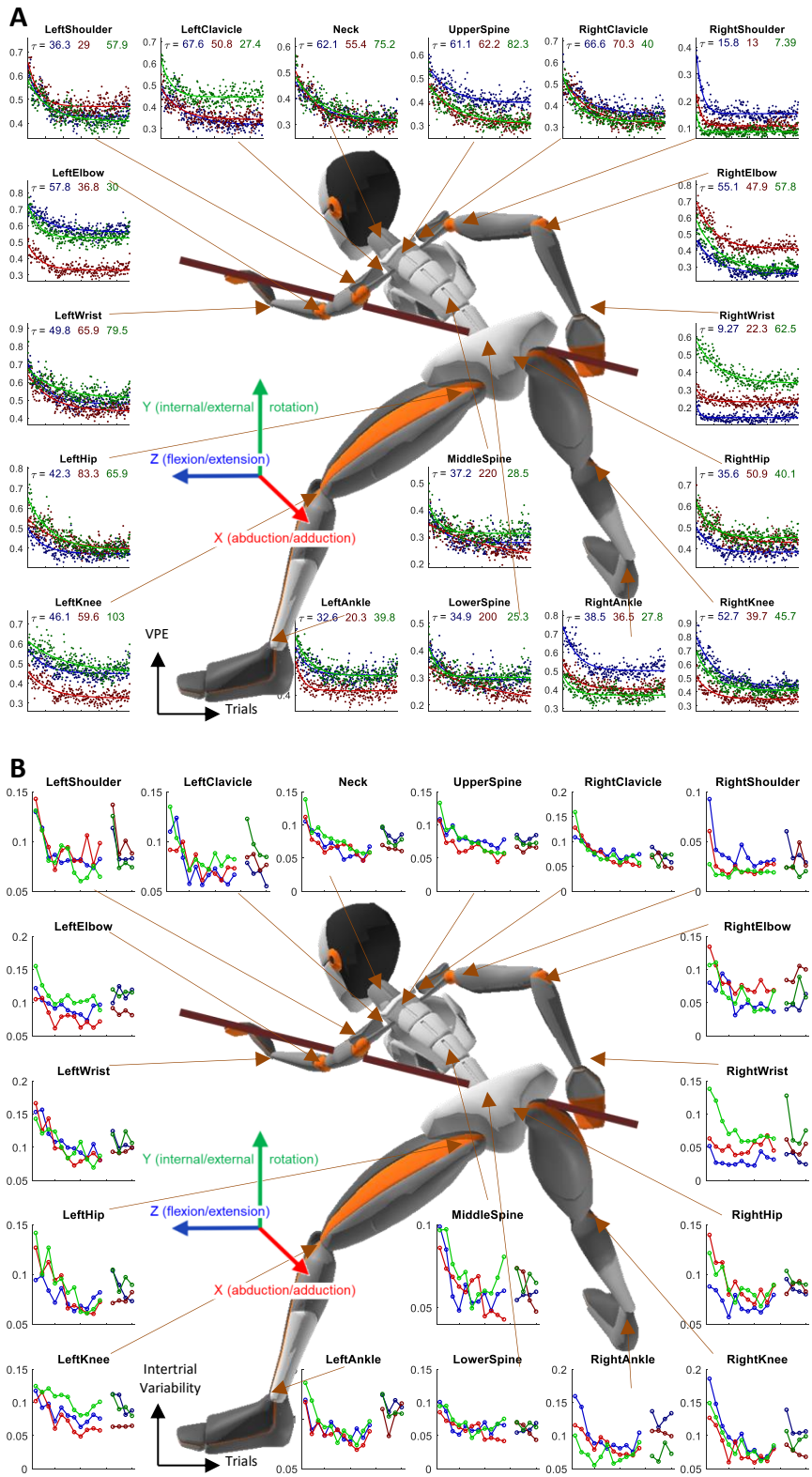

Figure 4. *Learning over Joints*. Velocity Profile Error (VPE) and Intertrial variability reduction across all joints. (**A**) The trial-by-trial VPE for all 3 DoF of all joints, averaged across all subjects, with an exponential fit. The time constants of the fits are reported under the title color coded for the DoF (blue: flexion/extension; red: abduction/adduction; green: internal/external rotation). (**B**) VPE intertrial variability over blocks of 25 trials, averaged across all subjects.

Inter-subject differences in variability and learning

We found significant differences between subjects in their initial errors, final errors, intertrial variability, and learning, which are overlooked in the group average results. One subject, who had low initial errors, showed no learning, i.e. did not reduce her error over trials from the first block (trials 1-25) to the learning plateau (trials 201-300). For all other subjects the final errors were smaller than the initial (Figure 5A). There was a significant correlation between the initial and the final errors (r=0.55, p=0.012), meaning subjects with higher initial errors tended to have higher final errors as well.

While over learning most subjects decreased their variability in the outcome (ball direction; Figure 1H & 5B) there was a clear tendency (though non-significant) for subjects who were initially more variable to be also more variable after learning (r=0.37, p=0.11; Figure 5B). In the joint movement variability, which also decreases over learning (Figure 4B), this tendency was also evident (Figure 5E & Fig 5E Supplement). While this phenomenon was observed in various joints across the body, and dominant in the abduction across the spine joints, it was most evident in the right shoulder abduction and rotation, the two joints that do most of the movement and carry most of its variance (Figure 2).

Learning was defined as the difference between the initial error (over the first block: trials 1-25) and the final error (over the learning plateau: trials 201-300) normalized by the initial error. There was no significant correlation between the learning and the final error, but there is a trend that more learning leads to smaller final errors (r=-0.1; Figure 5C). We tested if higher levels of initial task-relevant motor variability (variability in the directional error of the target ball) in this complex real-world task could predict faster learning across individual, as found in simple lab experiments (Wu et al., 2014). We indeed found that individuals with higher intertrial variability in the directional error of the target ball over the first block showed more learning (r=0.49, p=0.03; Figure 5D). Importantly, the intertrial variability was calculated over the residuals from a regression line fitted to the ball direction in the first block, to correct for the learning that is happening within the block. The uncorrected intertrial variability showed even stronger correlation with learning across subjects (r=0.67, p=0.001) and the subject who showed no learning is also the one with the lowest corrected variability. We further tested the link between learning and variability over the full body kinematics. We found that the only joint where the intertrial variability shows significant correlation to learning was the right elbow rotation (r=0.57, p<0.01; Figure 5F & Fig 5F Supplement). Thus, while learning leads to overall reduction in movement variability, only initial variability in specific, task-relevant, dimensions can facilitate/predict learning.

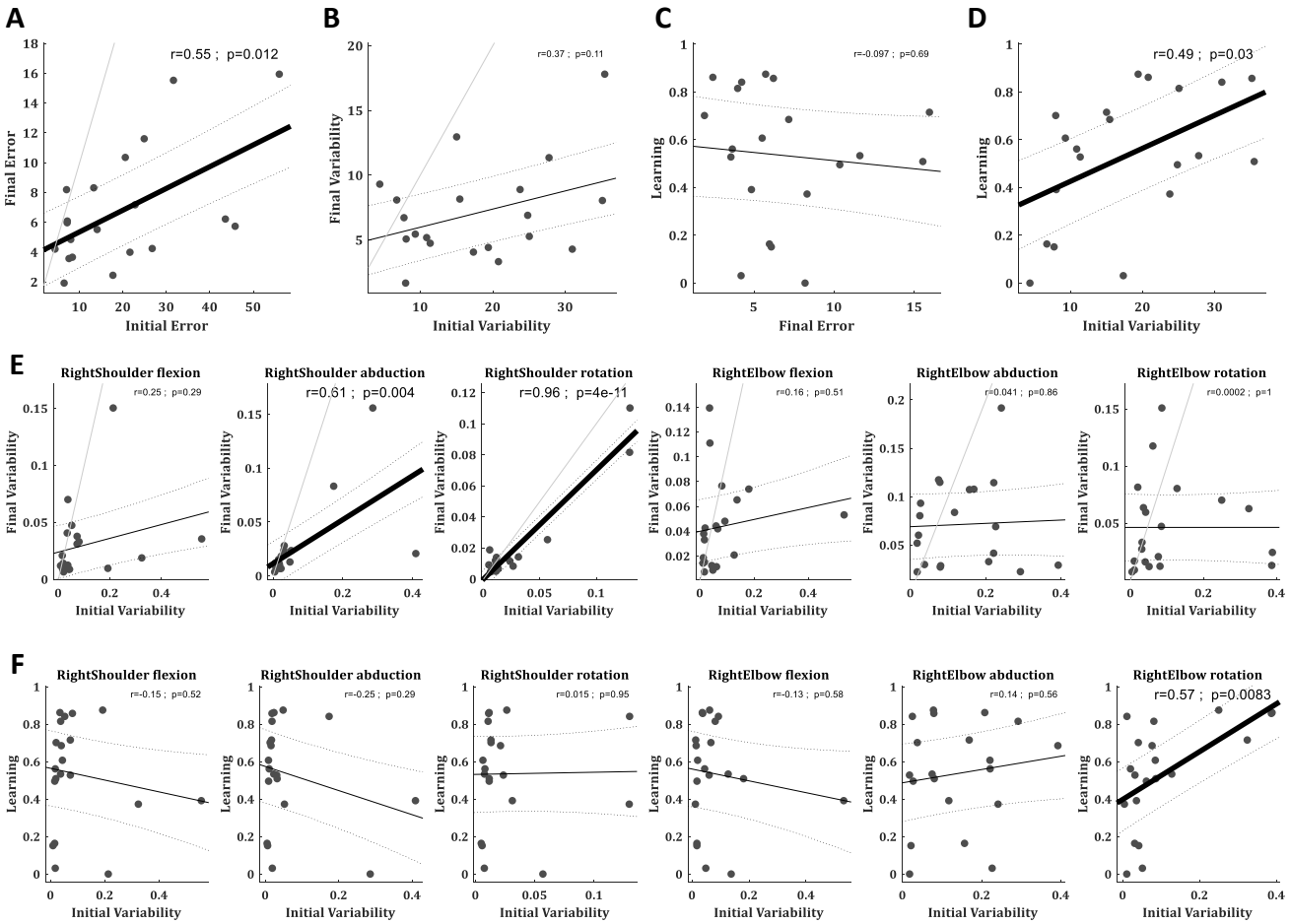

Figure 5. *Variability and learning across subjects*. (**A**) Correlation between subjects' mean absolute directional error over first block (trials 1-25) and over the learning plateau (trials 2001-300). (**B**) Correlation between subjects' directional variability over first block (corrected for learning trend, see text) and over the learning plateau (**C**) Correlation between subjects' mean absolute directional error over the learning plateau and their learning (**D**) Correlation between subjects' directional variability over first block (corrected for learning trend, see text) and their learning (**E**) Correlation between subjects' VPE variability over the first block and over the learning plateau for the right arm joints. (**F**) Correlation between subjects' VPE variability over first block and their learning for the right arm joints.

EEG activity reveals two types of learners

The most prominent feature of the EEG brain activity recorded in this study was the transient increase in beta oscillations across the sensorimotor network after the end of the movement, known as post-movement beta synchronization (Pfurtscheller et al., 1996) or post-movement beta rebound (PMBR; Figure 6A). While motor adaptation studies suggest the PMBR is attenuated by movement errors (e.g. Tan et al., 2014, 2016; Torrecillos et al., 2015), on average across subjects there is no clear trend of PMBR increase over learning, though the error decrease (Figure 6B). Testing for the PMBR increase (the difference between the final PMBR over the learning plateau: trials 201-300, and the initial PMBR over the first block: trials 1-25) over subjects reveals a more complex picture.

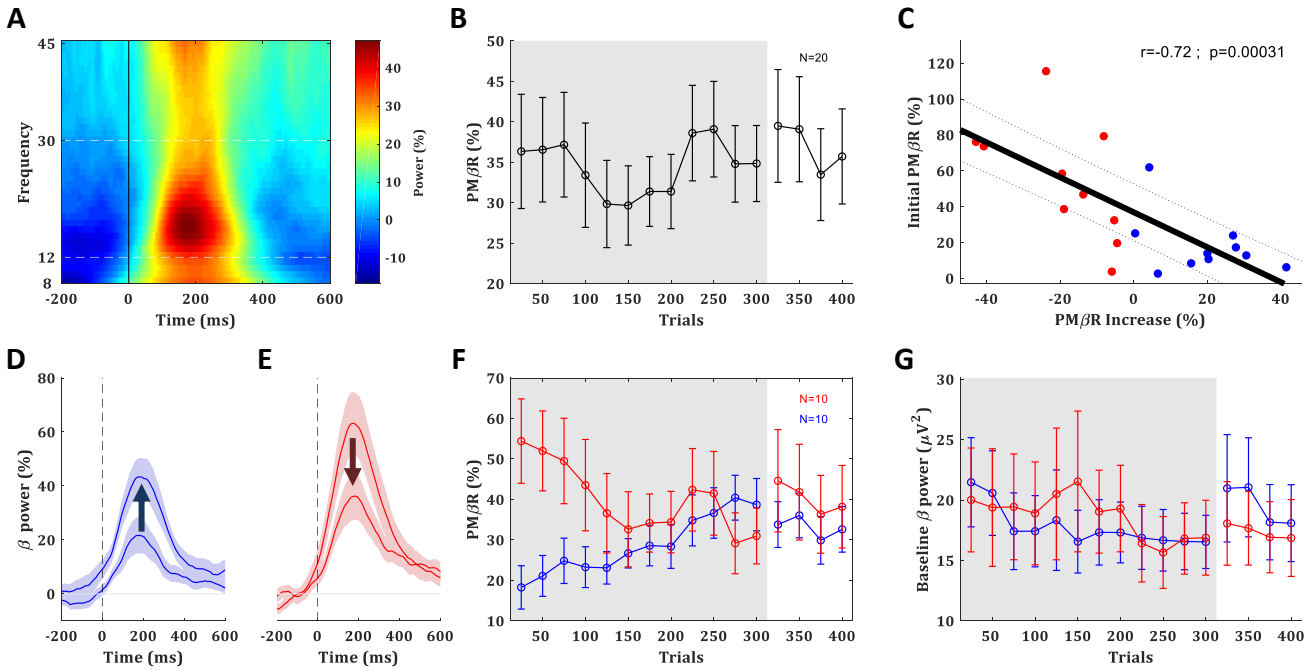

Figure 6. *Post-movement beta rebound*. (**A**) Time-frequency map of a typical subject aligned to movement offset (ball movement onset), obtained by averaging the normalized power over virtual electrode C3. the post movement beta rebound (PMBR) is clearly visible. (**B**) PMBR over blocks of 25 trials for the first (grey background) and the second (white background) target, averaged across all subjects, error bars represent SEM. (**C**) Subjects' PMBR increase from the first block (trials 1-25) to the learning plateau (trials 2001-300) vs their initial PMBR over the first block. Subjects are color coded relative to zero on the x-axis: subjects with a positive PMBR increase value are in blue (PMBR increasers) and subjects with a negative PMBR increase value are in red (PMBR decreasers). (**D,E**) Beta power profile over the first and last blocks to the first target for the PMBR increasers (D) and decreasers (E). The arrows mark the direction from first to last. Line is averaged across all subjects in the group and the light background mark the SEM. (**F,G**) PMBR (F) and Baseline beta power (G) of the increasers (blue) and decreasers (red) over blocks of 25 trials for the first (grey background) and the second (white background) target, averaged across all subjects in each groups, error bars represent SEM.

While half of the subjects do show an increase in the PMBR over learning, the other half shows a decrease (Figure 6C). This was negatively correlated with the initial PMBR ($r=-0.72$, $p<0.001$), i.e. subjects who had higher initial PMBR had higher decrease (or lower increase) in PMBR over learning. Thus, the beta-power time courses over the first and last blocks of the learning shows a strong increase for one group (Figure 6D) and a strong decrease for the other (Figure 6E). The first group shows a clear trend of PMBR increase over learning, in consistent with previous adaptation studies, while the second group shows clear trend of PMBR decrease over learning (Figure 6F).

Since the beta-power changes were calculated as percent signal change relative to the average power over the block, these group differences could potentially be driven by differences in the baseline. Importantly, this is not the case as there is no real difference in the baseline between the groups, not in the values nor in the trend over learning (Figure 6G).

This clear grouping in the EEG data requires an inquiry for potential group differences in the movement data. While there seems to be no difference in the initial error between the groups, the PMBR decreasers are faster initial learners, as evident by the exponential learning curve fits for the decay in the directional error of the target ball for the two groups. The PMBR increasers group

is best described by a single exponential learning curve with a time constant of 47 trials (Figure 7A), while the PMBR decreasers group is best described by a double exponential learning curve with a fast time constant of 7.75 trials and a slow one of 178 trials (Figure 7B).

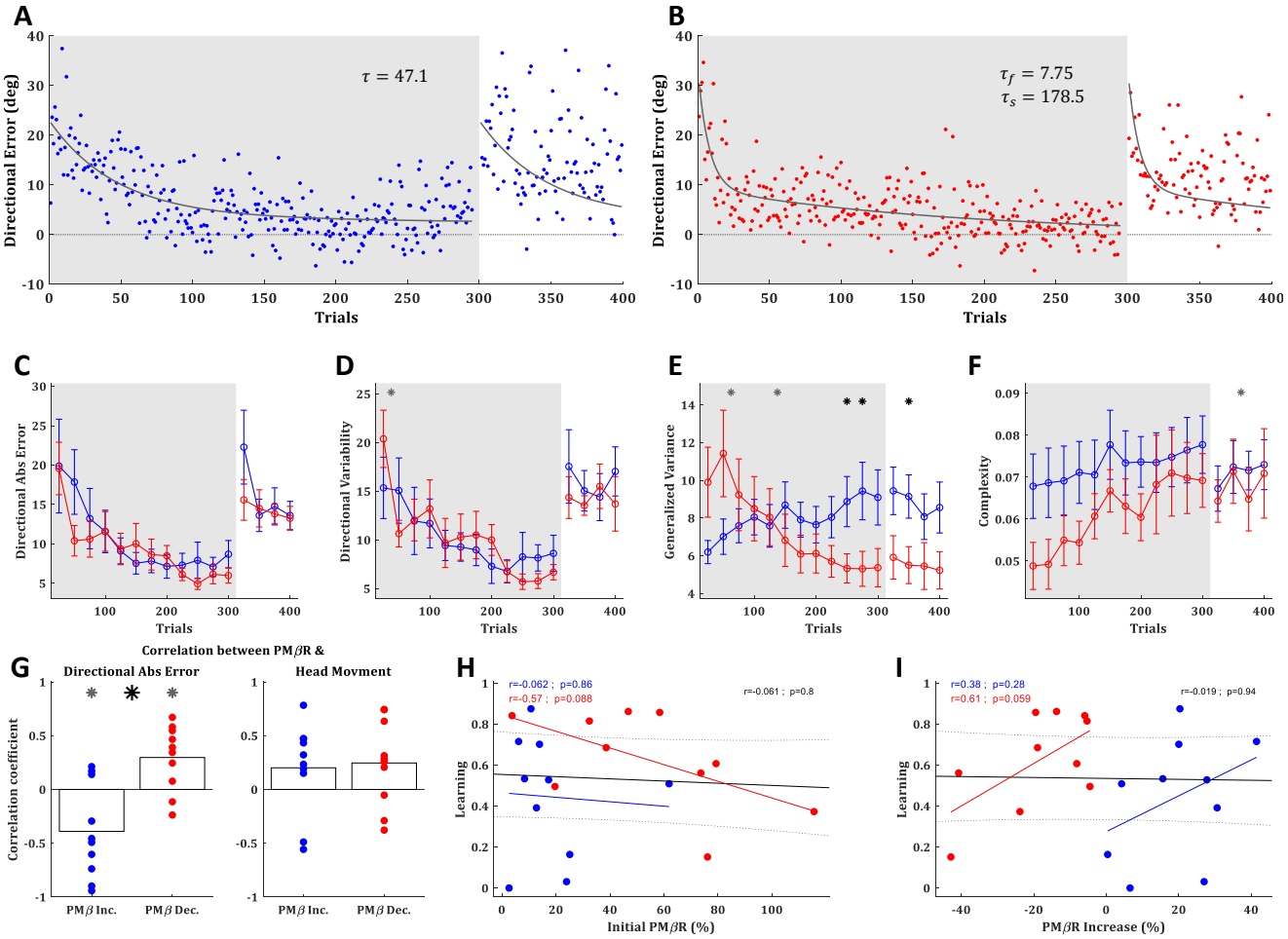

Figure 7. *PMBR predict learning mechanism*. **(A,B)** The trial-by-trial directional error of the target-ball (relative to the direction from its origin to the centre of the target pocket) for the first (grey background) and the second (white background) target, averaged across subjects in each group, PMBR increasers in blue (**A**) and decreasers in red (**B**), with a double-exponential fit (grey curve). The trials to the second target are also presented with the curve of the fit to the first target. **(C-F)** Directional absolute error (**C**), directional variability (**D**), generalized variance (**E**), and manipulative complexity (**F**) of the PMBR increasers (blue) and decreasers (red) over blocks of 25 trials for the first (grey background) and the second (white background) target, averaged across all subjects in each groups, error bars represent SEM. Black asterisks indicate significant difference between the groups in the block. Grey asterisks indicate significant difference between the groups in the change between blocks. (**G**) The correlation coefficients between the PMBS and absolute directional error (right panel) and Head movements (left panel) for all subjects. Grey asterisks indicate group correlations significantly different than zero. Black asterisk indicate significant difference in the correlation coefficients between the groups. (**H,I**) Correlations between the initial PMBR (**H**) and the PMBR increase (**I**) to the overall learning, across all subjects (black) and within each group (blue: increases ; red: decreases).

This group difference is evident in the decrease in error magnitude from the first block to the second (Figure 7C), thought Student's t test found no significant differences between the groups (p=0.12). PMBR decreasers also seem to modify their variability (actively control of the exploration-exploitation trade-off, explicitly or implicitly) to improve learning, as evidenced by their high variability in the first block and the very steep decrease towards the second (Figure 7D). This steep trend was significantly different from that of the PMBR increasers group (p=0.015). The

dynamical control of the variability was even more significantly evident in their full-body movement. The trend of the GV over the velocity profiles of all joints, which increases fast over the first ~40 trials and later decreases slowly (Figure 4A), is evident only in this group, while the other group (PMBR increasers) shows a slow gradual increase in their GV (Figure 7E). Lastly, PMBR increasers tend to have higher complexity in their movement (used more DoF), especially in the early blocks as the PMBR decreasers had a steeper increase in complexity and towards the end of the learning there was no difference between the groups (Figure 7F).

Within subject, the PMBR decreasers showed significant negative correlation over blocks between the directional error and the PMBR (mean correlation: r=-0.39, t test p=0.02), while the PMBR increasers shows significant positive correlation (mean correlation: r=0.3, t test p=0.013; Figure 7G), leading to a very significant difference between the groups (t test p<0.001). As additional control we also looked for correlation over blocks between the PMBR and the peak head acceleration during the same time interval as a control for head movements contamination of the PMBR effect. Here we found no correlation for either of the groups (mean correlation: r=0.20, t test p=0.17 and r=0.25, t test p=0.09, for the PMBR increasers and decreasers respectively), and more importantly, no difference between the groups (t test p=0.81).

Finally, we explored the correlation between PMBR and learning. Across all subjects, we found no correlation between the learning rate and the initial PMBR (r=-0.06; Figure 7H) or the PMBR increase (r=0.02; Figure 7I). When considering each group separately, there was still no correlation between the learning rate and initial PMBR for the PMBR increasers (r=-0.06) and a trend of negative correlation for the PMBR decreasers (r=-0.57, p=0.088). But, the PMBR increase showed a clear positive correlation trend with learning for both groups (r=.38, p=0.28 and r=.61, p=0.059, for the PMBR increasers and decreasers respectively; Figure 7I). Meaning, for the PMBR increasers, more increase suggests more learning; for the PMBR decreasers, less decrease suggests more learning.

Discussion

In this paper, we introduce a new paradigm for studying naturalistic motor learning during whole-body movement in a complex real-world motor skill. Our results present new insights into motor learning in the real-world. While the learning curves in this in-the-wild paradigm are within the same range of those reported in reductionistic motor adaptation tasks (e.g. McDougle et al., 2015; Smith et al., 2006) the movement and the learning structures are more complex. Most importantly, our neural recording reveals two types of motor learners: PMBR increasers and PMBR decreasers. While these groups are defined by their patterns of beta oscillations, there are clear behavioral differences between these groups: PMBR decreasers have faster initial learning, they

effectively modulate their movement variability for that, and use fewer DoF. These is the first study to report such neurobehavioral identification of two types learners.

Fundamentals of real-world motor learning

Across all subjects, we find that motor learning is a holistic process - the entire body is learning the task. This was as evident in the decrease in the VPE and in the intertrial variability over learning (Figure 4). This should not come as a surprise, considering decades of research in sport science showing this relation (for example, baseball pitcher's torso, pelvis, and leg movements are directly associated with ball velocity (Kageyama et al., 2014; Oliver and Keeley, 2010; Stodden et al., 2006)). And yet, unlike baseball pitches or basketball throws where the whole body is moving, in a pool shot the shooting arm is doing most of the movement and there is very little body movement. Thus, the whole-body learning is not trivial and suggestive that even in arm movement learning tasks there is a whole-body learning aspect which is overlooked.

We also found a proximal-to-distal gradient in the learning rates over the right arm joints (Figure 4A). This is especially interesting in light of the well-known phenomenon of proximal-to-distal sequence in limb movements in sports science (Herring and Chapman, 1992) and in rehabilitation (Twitchell, 1951). In sports science, the phenomenon is dated to the earliest known instructions for playing golf, written by Thomas Kincaid in 1687: *"All motions with the strongest joynts performe; Lett the weaker second and perfect the same"* (cited in Herring and Chapman, 1992). In modern sport science it addressed as sequential order of joints movements initiation (or in reaching peak velocity) from the proximal joints to the more distal ones, which are lagging behind their proximal neighbors. While there are records of proximal-to-distal sequence at multiple time scales (Serrien and Baeyens, 2017), our results are the first to suggest that this gradient also occur over reputation as part of the learning process. This actually follows the same logic of Kincaid: proximal joints learn and stabilize earlier while distal joints keep learning and adapting for fine tuning - *"perfect the same"*.

Variability & learning

Intertrial variability is a fundamental characteristic of human movements and its underling neural activity (for review see Faisal et al., 2008). It was recently reported that individuals exhibit distinct magnitudes of movement variability, which are consistent across movements and effectors, suggesting an individual traits in movement variability (Haar et al., 2017). Our results show that subjects who were initially more variable tended to be also more variable after learning in many joints across the body (Figure 5E & Fig 5E Supplement) including the right shoulder and wrist. This supports the notion that there is an individual trait in movement variability.

Intertrial kinematic variability is also thought to be critical for motor learning (e.g., Braun et al., 2009; Dhawale et al., 2017; Herzfeld and Shadmehr, 2014; Teo et al., 2011; Wilson et al., 2008). It was suggested individuals with higher levels of task-relevant movement variability exhibit

faster motor learning in both reinforcement learning and motor adaptation error-based paradigms (Wu et al., 2014). The failures to reproduce this result in visuomotor adaptation studies (He et al., 2016; Singh et al., 2016), led to the idea that experiments with task-relevant feedback (which is common in visuomotor studies) emphasize execution noise over planning noise, whereas measurements made without feedback (as in Wu et al., 2014) may primarily reflect planning noise (Dhawale et al., 2017). This is in-line with a recent modeling work in a visuomotor adaptation study in which subjects with higher planning noise showed faster learning, but movement variability (with feedback) was dominated by execution noise (van der Vliet et al., 2018). In our task there were no manipulations or perturbations, thus, task-relevant feedback was fully available to the participants. On the other hand, in real-world there is no baseline variability, and the variability was measured during early learning and therefore is probably dominated by planning noise, regardless of the visual feedback. Indeed, subjects with higher variability in the target ball direction over the first block showed higher learning rates (Figure 5D). Our results straighten the link between variability and learning and are the first to show that it applies also to real-world tasks. We also found that the only joint angle that shows significant correlation between learning and initial variability is the right elbow rotation (Figure 5F & Fig 5F Supplement). Following the idea that task-relevant variability is what predicts learning, it would suggest that the elbow rotation is the most important joint angle to adjust during initial learning of a simple pool shoot. Indeed, guide books for pool and billiards emphasize that when shooting, one should keep one's body still and move only the back (right) arm from the elbow down. While the flexion movement is the one that give the power to the shoot, the arm supination (also known as 'screwing' in billiards, and measured by the elbow rotation in our IMUs setup) maintains the direction of the cue.

EEG activity predicts differences in motor learning strategy

Most previous studies that looked for neural signatures of human motor learning used MRI and focused on functional and anatomical brain changes following learning and not during learning (e.g. Haar et al., 2015; Hecht et al., 2014; Hlustik et al., 2004; Sampaio-Baptista et al., 2015; Scholz et al., 2009; Wiestler and Diedrichsen, 2013). While MRI has better spatial resolution than EEG it has poor temporal resolution, and more importantly, real-world motor tasks cannot be done in the MRI scanner. Thus, the move from the MRI environment to wireless EEG recordings enables study of human brain responses in a real-world task during the motor learning process itself.

Beta oscillations (13–30 Hz), which are related to GABAergic activity (Hall et al., 2010, 2011; Roopun et al., 2006; Yamawaki et al., 2008), are a key neural feature of the sensorimotor system, that can be measured with EEG. More specifically, there is transient and prominent increase in beta oscillations across the sensorimotor network after cessation of voluntary movement known as post-movement beta rebound (PMBR) or post-movement beta synchronization (Pfurtscheller et al., 1996). PMBR is thought to signal GABA concentration, as measured by magnetic resonance spectroscopy (MRS; Cheng et al., 2017; Gaetz et al., 2011).

In the EEG data recorded during real-world motor learning in the current study, we found two groups of subjects: PMBR increasers and decreasers. The first group had low initial PMBR amplitudes and showed an increase over learning as subjects reduced their error, while the second group had high initial PMBR amplitudes and showed a decrease over learning. While there were no differences between these groups in their initial and final errors or in the total learning, there were clear behavioral differences during learning between the groups that suggest that the groups use different learning mechanisms. PMBR decreasers were more strategic learners. They showed an increase followed by decrease in the overall variability of their movement (GV; Figure 7C) which is suggestive of an active control of the exploration-exploitation trade-off, which suggest they used model-free reinforcement learning (Phillips et al., 2011) and not only error-based adaptation. They also showed higher initial variability in the direction of the target ball which is quickly suppressed (Figure 7B) in a way that farther support this idea of active control and enable faster initial learning.

In motor adaptation studies, PMBR was reported to negatively correlate with movement errors, lower errors induced higher PMBR (e.g. Tan et al., 2014, 2016; Torrecillos et al., 2015), and therefore to increase over learning. On the other hand, in a force tracking task PMBR decreased with learning (Kranczioch et al., 2008). Additionally, PMBR is positively correlated with MRS-measured GABA concentration (Cheng et al., 2017; Gaetz et al., 2011) which are decreasing over sequence learning in force tracking (Floyer-Lea et al., 2006) and serial reaction time (Kolasinski et al., 2019) tasks. The motor learning literature traditionally classified its toy tasks into two broad categories: motor adaptation and motor sequence learning, and suggest different learning process for these categories (Doyon and Benali, 2005; Doyon et al., 2003). Recent literature addresses it in terms of the learning mechanisms as adaptation versus de-novo learning (Sternad, 2018; Telgen et al., 2014; Yang et al., 2018). With either definition, the studies mentioned above fall nicely into the different categories, where the adaptation studies showed PMBR increase and the de-novo learning studies showed decrease in PMBR (or MRS-measured GABA). Thus, there are probably different GABAergic mechanism in adaptation and de-novo learning, which are evident in the PMBR and the MRS-measured GABA in these studies.

Reductionistic toy paradigms emphasize a specific type of learning for all subjects, such as motor adaptation, whereas real-world motor learning involves multiple high- and low-level learning mechanisms, where different subjects might emphasize one learning modality over the other. In our real-world learning paradigm, subjects performed error-based adaptation as they learned from the directional error of the target ball in each trial, but they also performed de-novo learning as they learned to use the cue and to sequence their movement over joints when making a shot. We speculate that the PMBR increasers mostly learned from their error in a classical motor adaptation approach, and thus showed similar neural patterns to the ones recorded in motor adaptation paradigms, while the PMBR decreasers, being more strategic in their learning (as evident from the

behavioral differences between the groups), used de-novo learning to build a new controller for moving their body and the cue stick in the context of the task, and thus showed a neural pattern which reflects de-novo learning tasks.

Further support for this difference in mechanism can be found in the first block to the second target. In toy-tasks, after-effects are considered a benchmark for adaptation that is absent in de-novo learning (Yang et al., 2018). While there are no after-effects in our task, as there is no perturbation, the errors on the first block to the second target can serve for the same dissociation as de-novo learning should induce general improvement on the task, whereas adaptation would be specific to the learned target. Indeed, the PMBR increasers showed the same errors on the first block to the second target as they had to the first block while the PMBR decreasers shows smaller errors to the second target.

Conclusions

In this study we demonstrate the feasibility and importance of studying human neuroscience in-the-wild, and specifically naturalistic real-world skilled tasks. While we find similarities in learning structures between our real-world paradigm and traditional, reductionistic learning studies, we highlight crucial differences: namely, real-world motor learning is a holistic full-body mechanism across the entire body, and involves multi-modal learning mechanisms which subjects have to combine in new ways when faced with the complexity of learning in the real world, and different types of subjects will have to emphasize one over the other.

Online Methods

Experimental Setup and Design. 20 right-handed healthy human volunteers with normal or corrected-to-normal visual acuity (10 women and 10 men, aged 24±2) participated in the study. The volunteers, who had little to no previous experience with playing billiards, came to the lab to play billiards. Each subject performed 300 repeated trials where the white ball and the target ball were placed in the same locations and the subject was asked to shoot the target ball towards the pocket of the far-left corner, followed by an additional 100 trials where the balls were placed in the same locations and the subject were asked to shoot towards the pocket of the far right corner (Figure 1A). The trials were split into 8 sets of 50 trials (6 sets to the first pocket and 2 sets to the second) with a short break in-between. For the data analysis we further split each set into two blocks of 25 trials each, resulting in 12 blocks to the first pocket and 4 blocks to the second. During the entire learning process, we recorded the subjects' full body movements with a motion tracking 'suit' of 17 wireless inertial measurement units (IMUs; Figure 1B), and their brain activity with a wireless EEG headset (Figure 1C). The balls on the pool table were tracked with a high-speed camera (Dalsa Genie Nano) to assess the subjects' success in the game and to analyze the changes throughout

learning, not only in the body movement and brain activity but also in its outcome – the ball movement (Figure 1D).

Full-Body Motion Tracking. Kinematic data were recorded at 60 Hz using a wearable motion tracking 'suit' of 17 wireless IMUs (Xsens MVN Awinda, Xsens Technologies BV, Enschede, The Netherlands). Data acquisition was done via a graphical interface (MVN Analyze, Xsens technologies BV, Ensched, The Netherlands). The Xsens joint angles and position data were exported as XML files and analyzed using a custom software written in MATLAB (R2017a, The MathWorks, Inc., MA, USA). The Xsens full body kinematics were extracted in joint angles in 3 degrees of freedom for each joint that follow the International Society of Biomechanics (ISB) recommendations for Euler angle extractions of Z (flexion/extension), X (abduction/adduction) Y (internal/external rotation).

Movement Velocity Profile Analysis. From the joint angles we extracted the velocity profiles of all joints in all trials. We defined the peak of the trial as the peak of the average absolute velocity across the DoFs of the right shoulder and the right elbow. We aligned all trials around the peak of the trial and cropped a window of 1 sec around the peak for the analysis of joint angles and velocity profiles.

EEG acquisition and preprocessing. 14 channel EEG data were recorded at 256Hz using a wireless EEG system (Emotiv EPOC+, Emotiv, Inc., CA, USA). EEG signals were preprocessed in EEGLAB (https://sccn.ucsd.edu/eeglab; Delorme and Makeig, 2004). EEG signals were first high-pass filtered at 0.5 Hz using a basic FIR filter. Line noise at 50 Hz and its second harmonics at 100 Hz were removed by the Cleanline EEGLAB plug-in which adaptively estimates and removes sinusoidal artifacts using a frequency-domain regression technique (Mitra and Bokil, 2009). EEG signals were decomposed into independent component (IC) and artifacted ICs were removed with ADJUST, an EEGLAB plug-in for automatic artifact detection (Mognon et al., 2011). C3 electrode was interpolated from the recorded channels with spherical splines using EEGLAB 'eeg_interp' function.

EEG time-frequency analysis. Each block was transformed in the time-frequency domain by convolution with the complex Morlet wavelets in 1 Hz steps. Event-related EEG power change was subsequently calculated as the percentage change by log-transforming the raw power data and then normalizing relative to the average power calculated over the block, as no clear baseline could be defined during the task (Alayrangues et al., 2019; Tan et al., 2014, 2016; Torrecillos et al., 2015), and then subtracting one from the normalized value and multiplying by 100. Event-related power changes in the beta band (13–30 Hz) were investigated. Since it is a free behavior study there was no go cue and the subject shooted when they wanted. As a result, the best-defined time point during a trial is the end of the movement, defined by the beginning of the cue ball movement. Thus, the post-movement beta rebound (PMBR) was defined as the average normalized power over a 200ms

window centered on the peak of the power after movement termination (Tan et al., 2016). The PMBR was calculated for each individual trial before averaging over blocks for further analysis. The time frequency analysis was performed with custom software written in MATLAB (R2017a, The MathWorks, Inc., MA, USA).

References

Alayrangues, J., Torrecillos, F., Jahani, A., and Malfait, N. (2019). Error-related modulations of the sensorimotor post-movement and foreperiod beta-band activities arise from distinct neural substrates and do not reflect efferent signal processing. Neuroimage *184*, 10–24.

Belić, J.J., and Faisal, A.A. (2015). Decoding of human hand actions to handle missing limbs in neuroprosthetics. Front. Comput. Neurosci. *9*, 27.

Braun, D. a, Aertsen, A., Wolpert, D.M., and Mehring, C. (2009). Motor Task Variation Induces Structural Learning. Curr. Biol. *19*, 352–357.

Cheng, C.H., Tsai, S.Y., Liu, C.Y., and Niddam, D.M. (2017). Automatic inhibitory function in the human somatosensory and motor cortices: An MEG-MRS study. Sci. Rep. *7*.

Clerget, E., Poncin, W., Fadiga, L., and Olivier, E. (2012). Role of Broca's Area in Implicit Motor Skill Learning: Evidence from Continuous Theta-burst Magnetic Stimulation. J. Cogn. Neurosci. *24*, 80–92.

Delorme, A., and Makeig, S. (2004). EEGLAB: an open source toolbox for analysis of single-trial EEG dynamics including independent component analysis. J. Neurosci. Methods *134*, 9–21.

Dhawale, A.K., Smith, M.A., and Ölveczky, B.P. (2017). The Role of Variability in Motor Learning. Annu. Rev. Neurosci. *40*, 479–498.

Diedrichsen, J., Hashambhoy, Y., Rane, T., and Shadmehr, R. (2005). Neural correlates of reach errors. J. Neurosci. *25*, 9919–9931.

Doyon, J., and Benali, H. (2005). Reorganization and plasticity in the adult brain during learning of motor skills. Curr. Opin. Neurobiol. *15*, 161–167.

Doyon, J., Penhune, V., and Ungerleider, L.G. (2003). Distinct contribution of the cortico-striatal and cortico-cerebellar systems to motor skill learning. Neuropsychologia *41*, 252–262.

Faisal, a A., Selen, L.P.J., and Wolpert, D.M. (2008). Noise in the nervous system. Nat. Rev. Neurosci. *9*, 292–303.

Faisal, A., Stout, D., Apel, J., and Bradley, B. (2010). The Manipulative Complexity of Lower Paleolithic Stone Toolmaking. PLoS One *5*, e13718.

Floyer-Lea, A., Wylezinska, M., Kincses, T., and Matthews, P.M. (2006). Rapid Modulation of GABA Concentration in Human Sensorimotor Cortex During Motor Learning. J. Neurophysiol. *95*, 1639–1644.

Gaetz, W., Edgar, J.C., Wang, D.J., and Roberts, T.P.L. (2011). Relating MEG measured motor cortical oscillations to resting γ-Aminobutyric acid (GABA) concentration. Neuroimage *55*, 616–621.

Haar, S., Donchin, O., and Dinstein, I. (2015). Dissociating Visual and Motor Directional Selectivity Using Visuomotor Adaptation. J. Neurosci. *35*, 6813–6821.

Haar, S., Donchin, O., and Dinstein, I. (2017). Individual Movement Variability Magnitudes Are Explained by Cortical Neural Variability. J. Neurosci. *37*, 9076–9085.

Hall, S.D., Barnes, G.R., Furlong, P.L., Seri, S., and Hillebrand, A. (2010). Neuronal network pharmacodynamics of GABAergic modulation in the human cortex determined using pharmaco-magnetoencephalography. Hum. Brain Mapp. *31*, 581–594.

Hall, S.D., Stanford, I.M., Yamawaki, N., McAllister, C.J., Rönnqvist, K.C., Woodhall, G.L., and Furlong, P.L.

(2011). The role of GABAergic modulation in motor function related neuronal network activity. Neuroimage *56*, 1506–1510.

He, K., Liang, Y., Abdollahi, F., Fisher Bittmann, M., Kording, K., and Wei, K. (2016). The Statistical Determinants of the Speed of Motor Learning. PLOS Comput. Biol. *12*, e1005023.

Hecht, E.E., Gutman, D.A., Khreisheh, N., Taylor, S. V., Kilner, J., Faisal, A.A., Bradley, B.A., Chaminade, T., and Stout, D. (2014). Acquisition of Paleolithic toolmaking abilities involves structural remodeling to inferior frontoparietal regions. Brain Struct. Funct. *220*, 2315–2331.

Herring, R.M., and Chapman, A.E. (1992). Effects of changes in segmental values and timing of both torque and torque reversal in simulated throws. J. Biomech. *25*, 1173–1184.

Herzfeld, D.J., and Shadmehr, R. (2014). Motor variability is not noise, but grist for the learning mill. Nat. Neurosci. *17*, 149–150.

Hlustik, P., Solodkin, A., Noll, D.C., and Small, S.L. (2004). Cortical plasticity during three-week motor skill learning. J. Clin. Neurophysiol. *21*, 180–191.

Howard, I.S., Wolpert, D.M., and Franklin, D.W. (2015). The Value of the Follow-Through Derives from Motor Learning Depending on Future Actions. Curr. Biol. *25*, 397–401.

Ingram, J.N., and Wolpert, D.M. (2011). Naturalistic approaches to sensorimotor control. Prog. Brain Res. *191*, 3–29.

Kageyama, M., Sugiyama, T., Takai, Y., Kanehisa, H., and Maeda, A. (2014). Kinematic and Kinetic Profiles of Trunk and Lower Limbs during Baseball Pitching in Collegiate Pitchers. J. Sports Sci. Med. *13*, 742–750.

Kolasinski, J., Hinson, E.L., Divanbeighi Zand, A.P., Rizov, A., Emir, U.E., and Stagg, C.J. (2019). The dynamics of cortical GABA in human motor learning. J. Physiol. *597*, 271–282.

Krakauer, J.W., Pine, Z., Ghilardi, M., and Ghez, C. (2000). Learning of visuomotor transformations for vectorial planning of reaching trajectories. J. Neurosci. *20*, 8916–8924.

Kranczioch, C., Athanassiou, S., Shen, S., Gao, G., and Sterr, A. (2008). Short-term learning of a visually guided power-grip task is associated with dynamic changes in EEG oscillatory activity. Clin. Neurophysiol. *119*, 1419–1430.

Ma, L., Narayana, S., Robin, D.A., Fox, P.T., and Xiong, J. (2011). Changes occur in resting state network of motor system during 4weeks of motor skill learning. Neuroimage *58*, 226–233.

Mazzoni, P., and Krakauer, J.W. (2006). An Implicit Plan Overrides an Explicit Strategy during Visuomotor Adaptation. *26*, 3642–3645.

McDougle, S.D., Bond, K.M., and Taylor, J.A. (2015). Explicit and Implicit Processes Constitute the Fast and Slow Processes of Sensorimotor Learning. J. Neurosci. *35*, 9568–9579.

Mitra, P., and Bokil, H. (2009). Observed Brain Dynamics.

Mognon, A., Jovicich, J., Bruzzone, L., and Buiatti, M. (2011). ADJUST: An automatic EEG artifact detector based on the joint use of spatial and temporal features. Psychophysiology *48*, 229–240.

Oliver, G.D., and Keeley, D.W. (2010). Pelvis and torso kinematics and their relationship to shoulder kinematics in high-school baseball pitchers. J. Strength Cond. Res. *24*, 3241–3246.

Ono, Y., Noah, J.A., Zhang, X., Nomoto, Y., Suzuki, T., Shimada, S., Tachibana, A., Bronner, S., and Hirsch, J. (2015). Motor learning and modulation of prefrontal cortex: an fNIRS assessment. J. Neural Eng. *12*, 066004.

Pfurtscheller, G., Stancák, A., and Neuper, C. (1996). Post-movement beta synchronization. A correlate of an idling motor area? Electroencephalogr. Clin. Neurophysiol. *98*, 281–293.

Phillips, H.N., Howai, N.A., Stan, G.-B. V, and Faisal, A.A. (2011). The implied exploration-exploitation trade-off in human motor learning. BMC Neurosci. *12*, P98.

Reis, J., Schambra, H.M., Cohen, L.G., Buch, E.R., Fritsch, B., Zarahn, E., Celnik, P.A., and Krakauer, J.W. (2009). Noninvasive cortical stimulation enhances motor skill acquisition over multiple days through an effect on consolidation. Proc. Natl. Acad. Sci. U. S. A. *106*, 1590–1595.

Roopun, A.K., Middleton, S.J., Cunningham, M.O., LeBeau, F.E.N., Bibbig, A., Whittington, M.A., and Traub,

R.D. (2006). A beta2-frequency (20-30 Hz) oscillation in nonsynaptic networks of somatosensory cortex. Proc. Natl. Acad. Sci. U. S. A. *103*, 15646–15650.

Sampaio-Baptista, C., Scholz, J., Jenkinson, M., Thomas, A.G., Filippini, N., Smit, G., Douaud, G., and Johansen-Berg, H. (2014). Gray matter volume is associated with rate of subsequent skill learning after a long term training intervention. Neuroimage *96*, 158–166.

Sampaio-Baptista, C., Filippini, N., Stagg, C.J., Near, J., Scholz, J., and Johansen-Berg, H. (2015). Changes in functional connectivity and GABA levels with long-term motor learning. Neuroimage *106*, 15–20.

Scholz, J., Klein, M.C., Behrens, T.E., and Johansen-Berg, H. (2009). Training induces changes in white-matter architecture. Nat Neurosci *12*, 1370–1371.

Serrien, B., and Baeyens, J.P. (2017). The proximal-to-distal sequence in upper-limb motions on multiple levels and time scales. Hum. Mov. Sci.

Shadmehr, R., and Mussa-Ivaldi, F.A. (1994). Adaptive representation of dynamics during learning of a motor task. J. Neurosci. *14*, 3208–3224.

Singh, P., Jana, S., Ghosal, A., and Murthy, A. (2016). Exploration of joint redundancy but not task space variability facilitates supervised motor learning. Proc. Natl. Acad. Sci. *113*, 14414–14419.

Smith, M.A., Ghazizadeh, A., and Shadmehr, R. (2006). Interacting adaptive processes with different timescales underlie short-term motor learning. PLoS Biol. *4*, e179.

Sternad, D. (2018). It's not (only) the mean that matters: variability, noise and exploration in skill learning. Curr. Opin. Behav. Sci. *20*, 183–195.

Stodden, D.F., Langendorfer, S.J., Fleisig, G.S., and Andrews, J.R. (2006). Kinematic Constraints Associated With the Acquisition of Overarm Throwing Part I. Res. Q. Exerc. Sport *77*, 417–427.

Tan, H., Jenkinson, N., and Brown, P. (2014). Dynamic Neural Correlates of Motor Error Monitoring and Adaptation during Trial-to-Trial Learning. J. Neurosci. *34*, 5678–5688.

Tan, H., Wade, C., and Brown, P. (2016). Post-Movement Beta Activity in Sensorimotor Cortex Indexes Confidence in the Estimations from Internal Models. J. Neurosci. *36*, 1516–1528.

Taylor, J. a, Krakauer, J.W., and Ivry, R.B. (2014). Explicit and implicit contributions to learning in a sensorimotor adaptation task. J. Neurosci. *34*, 3023–3032.

Telgen, S., Parvin, D., and Diedrichsen, J. (2014). Mirror Reversal and Visual Rotation Are Learned and Consolidated via Separate Mechanisms: Recalibrating or Learning De Novo? J. Neurosci. *34*, 13768–13779.

Teo, J.T.H., Swayne, O.B.C., Cheeran, B., Greenwood, R.J., and Rothwell, J.C. (2011). Human theta burst stimulation enhances subsequent motor learning and increases performance variability. Cereb. Cortex *21*, 1627–1638.

Thomik, A.A.C. (2016). On the structure of natural human movement. Imperial College London.

Torrecillos, F., Alayrangues, J., Kilavik, B.E., and Malfait, N. (2015). Distinct Modulations in Sensorimotor Postmovement and Foreperiod ⍰ -Band Activities Related to Error Salience Processing and Sensorimotor Adaptation. *35*, 12753–12765.

Twitchell, T.E. (1951). The restoration of motor function following hemiplegia in man. Brain *74*, 443–480.

van der Vliet, R., Frens, M.A., de Vreede, L., Jonker, Z.D., Ribbers, G.M., Selles, R.W., van der Geest, J.N., and Donchin, O. (2018). Individual Differences in Motor Noise and Adaptation Rate Are Optimally Related. Eneuro *5*, ENEURO.0170-18.2018.

Wiestler, T., and Diedrichsen, J. (2013). Skill learning strengthens cortical representations of motor sequences. 1–20.

Wilks, S.S. (1932). Certain Generalizations in the Analysis of Variance. Biometrika *24*, 471.

Wilson, C., Simpson, S.E., van Emmerik, R.E. a, and Hamill, J. (2008). Coordination variability and skill development in expert triple jumpers. Sports Biomech. *7*, 2–9.

Wolpert, D.M., Diedrichsen, J., and Flanagan, J.R. (2011). Principles of sensorimotor learning. Nat. Rev. Neurosci. *12*, 739–751.

Wu, H.G., Miyamoto, Y.R., Gonzales Castro, L.N., Ölveczky, B.C., and Smith, M.A. (2014). Temporal structure of motor vriability is dynamically regulated and predicts motor learning ability. Nat. Neurosci. *17*, 312–321.

Yamawaki, N., Stanford, I.M., Hall, S.D., and Woodhall, G.L. (2008). Pharmacologically induced and stimulus evoked rhythmic neuronal oscillatory activity in the primary motor cortex in vitro. Neuroscience *151*, 386–395.

Yang, C., Cowan, N., and Haith, A. (2018). Contrasting de novo learning with adaptation by the expression of aftereffects.

Yokoi, A., Arbuckle, S.A., and Diedrichsen, J. (2018). The role of human primary motor cortex in the production of skilled finger sequences. J. Neurosci. *38*, 1430–1442.

Supplementary Figures

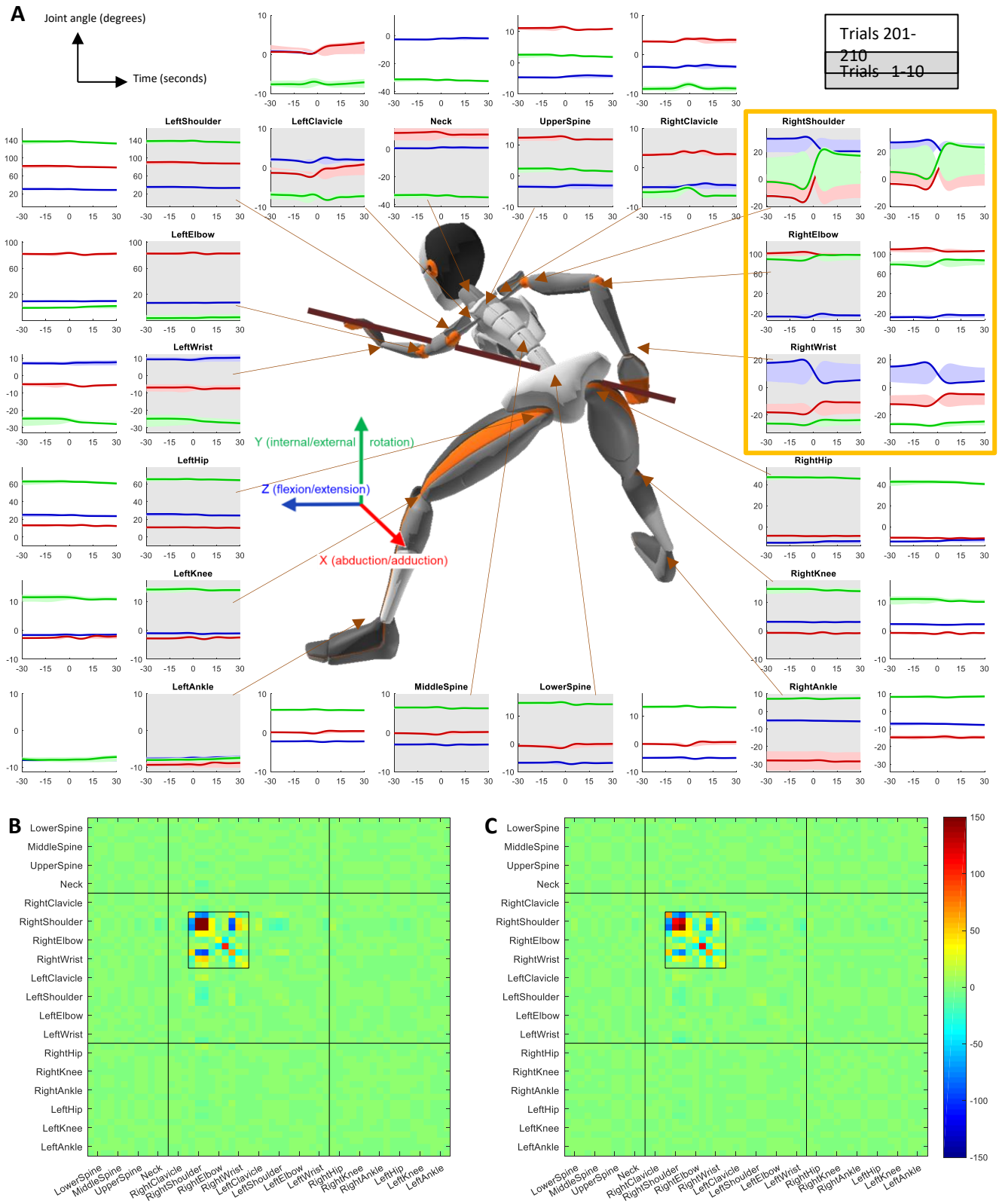

Figure 2 Supp. *Joint angles profiles and covariance*. (**A**) Joint angles profiles in 3 degrees of freedom for each joint (blue: flexion/extension, red: abduction/adduction; green: internal/external rotation) averaged across subjects and trials over the initial trials (1-10) in the inner circle (grey background) and after learning plateau (201-210) in the outer circle (white background). The joints of the right arm, which do most of movement in the task, are highlighted in orange box. (**B,C**) The variance covariance matrix of the joint angles profiles of all joints averaged across subjects and trials (**B**) over the initial trials (1-10) and (**C**) after learning plateau (201-210).

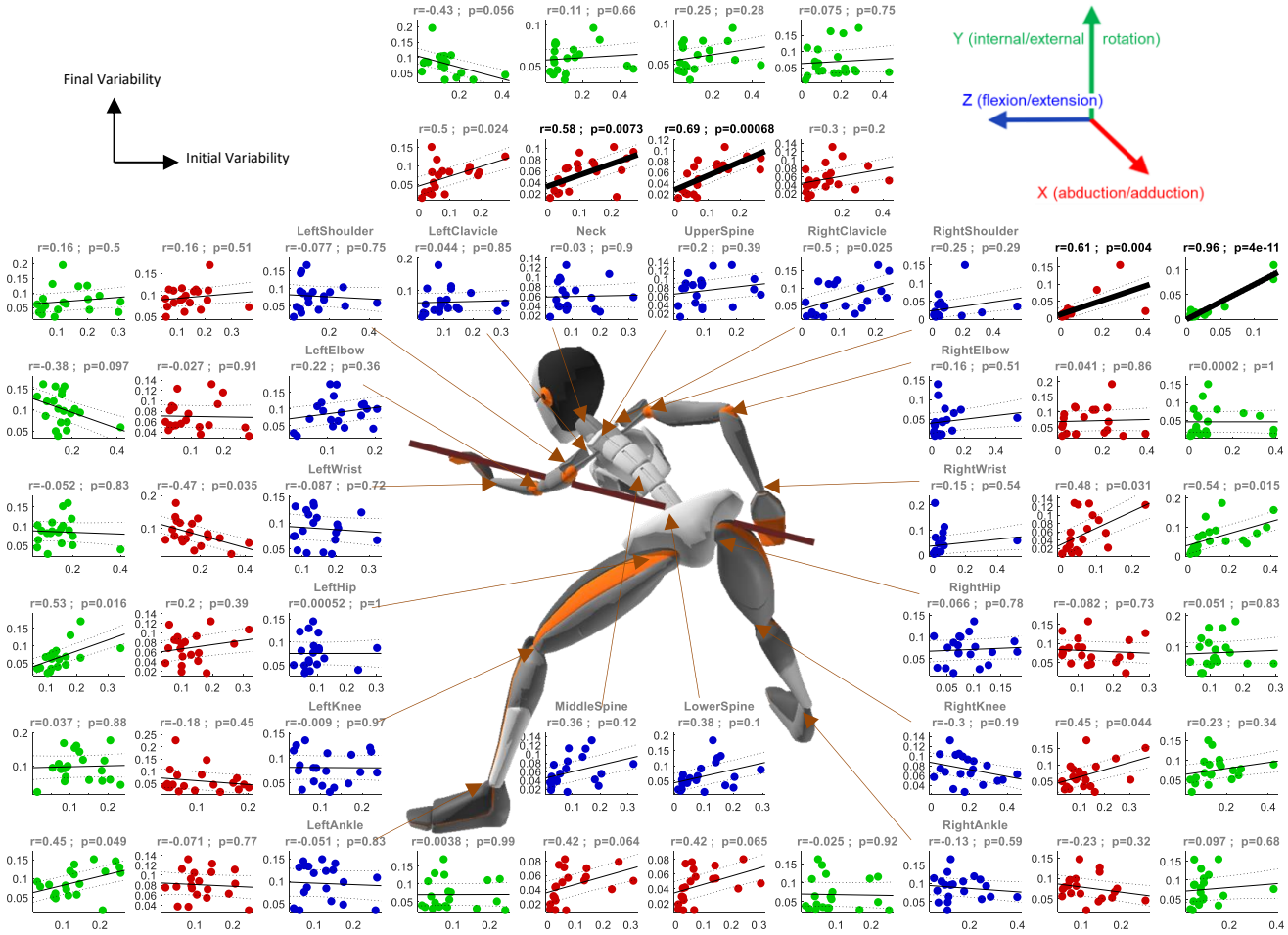

Figure 5E supp. Correlation between subjects' VPE variability over the first block and over the learning plateau, for all joints.

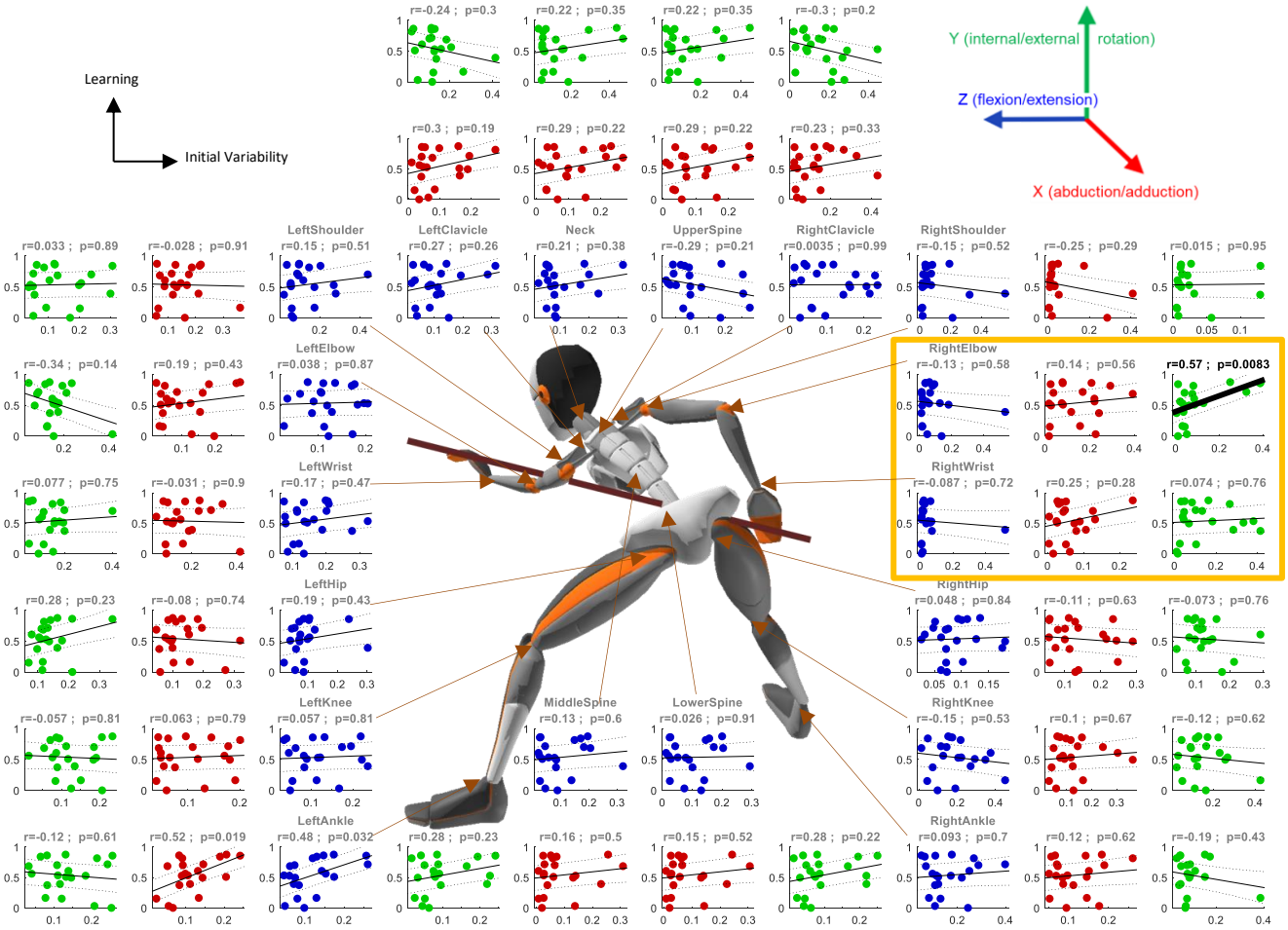

Figure 5F supp. Correlation between subjects' VPE variability over first block and their learning, for all joints.